



Reactivation of ancestral strains of HIV-1 in the gp120 V3 *env* region in patients failing antiretroviral therapy and subjected to structured treatment interruption

Wilson Pereira Silva^a, Domingos E.M. Santos^a, Elcio Leal^a, Adriana Brunstein^a,
Maria Cecilia A. Sucupira^a, Ester C. Sabino^b, Ricardo Sobhie Diaz^{a,*}

^a *Escola Paulista de Medicina, Universidade Federal de São Paulo, Rua Pedro de Toledo, 781-16 andar-CEP 04039-032, São Paulo, SP, Brazil*

^b *Fundação Pró-Sangue. Av. Dr. Enéas de Carvalho Aguiar, 155-1 andar-CEP 05403-000, São Paulo, SP, Brazil*

Received 16 January 2006; returned to author for revision 15 February 2006; accepted 19 April 2006

Available online 25 July 2006

Abstract

We analyzed gp120V3 HIV-1 *env* region genetic diversity of 27 patients failing antiretrovirals and subjected to 12-week structured treatment interruption (STI). Based on heteroduplex mobility assays, eight patients presented low pre- and post-STI genetic diversity (G1); five presented high pre-STI but low post-STI diversity (G2); five presented low pre-STI and high post-STI diversity (G3); and nine, high pre- and post-STI diversity (G4). One patient from G1, two from G2 and two from G3 were subjected to proviral DNA end-point PCR and sequencing. In three patients, the dramatic disturbance caused by STI resulted in ancestral viral progeny activation, which repopulated the cell reservoir. In two patients presenting highly homogeneous sequences and low immune selective pressure (dN/dS ratio <1), this phenomenon was not observed. The mechanisms involved in viral evolution, in which antiretroviral therapy also applies selective pressure, sometimes affects coreceptor usage of circulating viruses, leading to the suppression of ×4 strains.

© 2006 Published by Elsevier Inc.

Keywords: Structured treatment interruption; HIV-1; Envelope gene; Antiretroviral resistance

Introduction

Notorious for its genetic diversity, the HIV-1 genome generates all possible mutations on a continuous basis. This occurs as a result of the high rates of misincorporation by the reverse transcriptase ($\approx 4 \times 10^{-4}$ per replication cycle), the higher levels of viral replication and the size of genome ($\approx 10^{10}$ base pairs) (Mansky and Temin, 1995; Perelson et al., 1996). However, the viral population that seeds a new infection is usually highly homogeneous in both genotype and phenotype, and infection is followed by an increase in viral genetic diversity over time (Diaz et al., 1996; McNamee et al., 1992; Zhang et al., 1993; Zhu et al., 1993). The envelope gene encodes a

glycoprotein that is subjected to great selective pressure exerted by the immune system during chronic infection (Diaz et al., 1997; Zhang et al., 1997). The rate of evolution of this gene is approximately 1% per year (Diaz et al., 1997; Shankarappa et al., 1999), thereby generating the so-called viral quasispecies.

The viral phenotypes, which change during the course of HIV-1 infection, are classified as syncytium-inducing (SI) or non-syncytium-inducing (NSI) (Cheng-Mayer et al., 1990). There is a correlation between the phenotype, cytopathogenicity and cell tropism. The NSI phenotypes typically bind to the CCR5 chemokine receptors and present tropism for macrophages and monocytes, whereas SI phenotypes bind to CXCR4 and present tropism for lymphocytes (Roos et al., 1992; Zhu et al., 1993). The NSI phenotypes are present during primary infection and are less cytopathic, whereas SI phenotypes present greater potential for in vitro cell destruction and emerge over the course of infection (Koot et al., 1996; Shankarappa et al., 1999). Some authors have

* Corresponding author. Laboratório de Retrovirologia, R. Pedro de Toledo, 781, São Paulo, SP-04039-032, Brazil. Fax: +55 11 4192 3176.

E-mail address: rsdiaz@usp.br (R.S. Diaz).

shown a correlation between the emergence of SI viral phenotypes and disease progression (Koot et al., 1996; Shankarappa et al., 1999). The phenotype change requires mutation in the *env* gene. A change in the V3 loop amino acid charge from neutral or negative (D or E) to positive (R or K) at positions 306 or 320 leads the HIV-1 phenotype to change from NSI to SI (Fouchier et al., 1992).

The use of antiretroviral therapy leads to selective pressure similar to that exerted by the immune system. Because antiretroviral-resistant mutant viral strains are preexisting, subinhibitory levels of drugs increase the risk that such strains will be selected. In these cases, an accumulation of resistance mutations is followed by a decrease in the pharmacological activity of antiretroviral agents (Coffin, 1995; Larder and Kemp, 1989).

Resistance mutations also lead to a decrease in the replicative fitness of the virus (Goudsmit et al., 1997; Maeda et al., 1998; Martinez-Picado et al., 2000). In the absence of antiretroviral agents, the fitness of the wild-type virus is usually superior to that of the antiretroviral-resistant mutant virus. This phenomenon allows the reemergence of the wild-type virus in patients with resistant strain subjected to antiretroviral interruption. In studies of structured antiretroviral interruption (STI) in patients with virological failure, increased viral load and decreased CD4 counts have been observed simultaneous to the reversion of the antiretroviral resistance mutations (Deeks et al., 2001; Miller et al., 2000). In the present study, we analyzed the genetic diversity of the HIV-1 gp120 V3 *env* region in chronically infected patients subjected to a 12-week STI.

Results

Genetic characterization of HIV-1 populations

Proviral HIV-1 samples obtained from a group of 27 individuals subjected to an STI were screened by HMA. An intra-sample HMA was performed to evaluate the diversity within the quasispecies of each individual (Fig. 1). The PCR input, as estimated by end-point PCR and by real-time PCR DNA proviral load, was at least 50 copies (data not shown). We used the following definition criteria: sample showing only one band (homoduplex) was interpreted as having low diversity, reflecting a relative homogeneity of the proviral population; and sample showing a confluence of bands inferring more complex proviral quasispecies. According to these criteria, pre- and post-STI samples were analyzed, and the 27 individuals were divided into four groups: group 1 (patients 01, 07, 09, 13, 15, 20, 22 and 23), presenting little pre- or post-STI genetic diversity; group 2 (patients 03, 08, 19, 24 and 26), presenting high pre-STI but low post-STI genetic diversity; group 3 (patients 02, 04, 05, 10 and 25), presenting low pre-STI but high post-STI genetic diversity; and group 4 (patients 06, 12, 14, 16, 17, 18, 21, 27 and 28), presenting high pre- and post-STI genetic diversity. One patient from group 1 (patient 01), two from group 2 (patients 03 and 19) and two from group 3 (patients 04 and 05) were selected and subjected to a quasispecies analysis by proviral DNA genomic sequencing of the C2-V3-C3 gp120 region of the *env* gene.

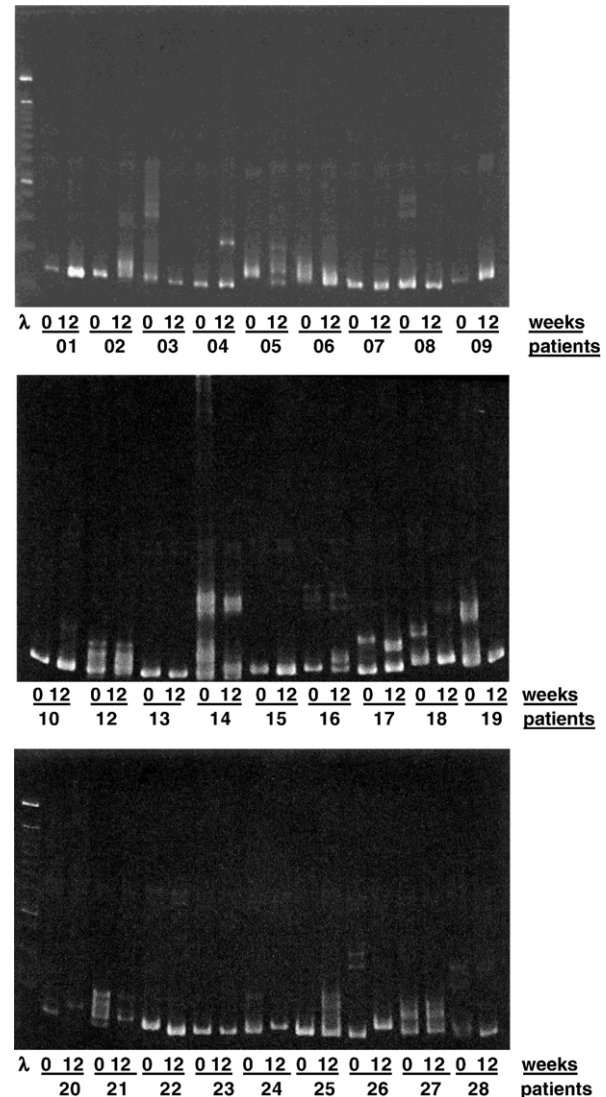


Fig. 1. HMA of pre-STI (week 0) and post-STI (week 12 of STI) samples from each patient. Molecular weight markers (labeled λ) are shown in the left-hand lanes of first and last gels.

Virologic and immunologic markers during STI

The 27 patients were experienced in all three classes of antiretrovirals, with a median of 8.9 prior ARV, ranging from 6 to 13. The median baseline HIV-1 RNA was 3.97 \log_{10} copies/mL, and the median baseline CD4+ cell count of 224 cells/mm³. Our results demonstrated an average reduction in CD4+ T cell count of 95 cells and an average increase of 0.64 \log_{10} in viral load, after 12 weeks of STI. Our results demonstrated an average reduction in T CD4+ of 95 cells and an average increase of 0.64 \log_{10} in viral load, after 12 weeks of STI. The CD4+ T cell counts and plasma HIV-1 viral loads during STI were studied in detail for five patients (patients 01, 03, 04, 05 and 19), and the results are depicted in Fig. 2. There was an increase in viral load and a decrease in CD4+ T cell count after the 12-week STI in patients 01, 05 and 19. No significant viral load increase was seen in patients 03 and 04 (less than 0.5 \log_{10} increase), although a significant decrease in CD4 count was documented.

Antiretroviral resistance-related mutations during STI

The evolution of the resistance mutation profile is depicted in Fig. 2. We generated *pol* sequences from plasma RNA and proviral DNA for all patients and there was a concordance in the resistance profile in both plasma and PBMCs either before or after STI. We did not observe mixed HIV populations in the resistance-related codons in any patient either before or after STI in plasma or PBMCs. Overall, resistance codons were replaced by wild-type codons, with the exception of the primary mutations in patient 19.

Genetic diversity of the C2-V3-C3 region

For each one of the five patients (patients 01, 03, 04, 05 and 19), we evaluated genetic diversity in the proviral quasispecies present in the pre- and post-STI samples. In samples from patients 01, 03 and 05, there were strong correlations between the HMA-inferred genetic diversity values and those measured by sequencing. The genetic diversity of clones found in pre-STI patient 01 samples (01A samples) was 0.00623 versus 0.00459 for those found in post-STI samples (01M samples). The dN/dS ratio for all patient 01 clones, according to the selected Goldman–Yang model (M0), was 0.1973, and there were no sites under positive selective pressure. For patient 03, genetic diversity of clones in the pre-STI samples (03A samples) was 0.05896, compared with 0.02942 for post-STI sample (03M sample) clones and 0.05182 for all clones combined. For this patient (patient 03), the M2 model was the best fit, and residues 291, 300, 302, 304, 320, 325 and 329 presented dN/dS ratios >1 (Fig. 3). There was no positive selection found in residues of patient 04 samples, in which the genetic diversity was 0.0107 in pre-STI samples (04A samples), 0.00791 in post-STI samples (04J samples) and 0.00959 on average. According to the Goldman–Yang model (M0), the mean dN/dS ratio in patient 04 samples was 0.4987. In patient 05 samples, the genetic diversity of clones was higher in post-STI samples (05L samples). Clones found in pre-STI patient 05 samples (05A samples) presented a genetic diversity of 0.0179 versus 0.0812 for those in post-STI samples (05L samples) and 0.0422 for all clones combined. For this patient (patient 05), M2 was selected, and we found dN/dS ratios >1 in residues 304, 306, 319, 321, 324, 345, 352, 353, 354, 356 and 359 (Fig. 3). The highest number of residues under positive selective pressure was found in patient 19 samples. For the quasispecies in PBMCs, we found a genetic diversity of 0.0363 for the pre-STI clones (in 19A samples), and 0.0312 for clones post-STI (19H samples). For quasispecies in plasma, we found the genetic diversity to be 0.0277 for clones in pre-STI samples (19Ar samples), 0.0194 for clones in samples collected after 1 week of STI (19Br samples) and 0.0482 for clones in post-STI samples (19Hr samples). According to the model M3, this patient (patient 19) presented high numbers of residues under positive selective pressure. In patient 19 PBMC samples, residues 278, 291, 293, 297, 334, 335, 338, 349, 351, 352 and 359 presented dN/dS ratios >1, and the majority of those residues (residues 278, 293, 334, 335, 338, 349, 352, 353 and

359) also presented dN/dS ratios >1 in patient 19 plasma samples.

Phylogenetic and coalescent analysis

In an attempt to better clarify the clustering pattern and the ancestral recrudescence, we performed phylogenetic and coalescent analyses. The sequences collected pre-STI were identified by grey circles, the sequences from post-STI were identified by black circles. The maximum likelihood trees constructed with the gp120 V3 *env* region of patients 03, 05 and 19 showed a similar topology clustering the sequences in two distinct groups (Figs. 4–6). The clustering pattern was strongly related to the STI status of sequences, in this way sequences from pre-STI clustered in a group whereas sequences from post-STI cluster in another distinct group. Because this bipolarity of the pre- and post-STI sequences was consistently observed in patients 03, 05 and 19, we then rooted the trees at the midpoint root that most likely will represent the ancestor of all sequences for each patient. This temporal pattern of the trees allowed us to estimate the distance of each cluster to the root. The post-STI clusters (cluster M in patient 03, cluster I in patient 05 and clusters GW1 and GW2 in patient 19) were located closer to the midpoint root whereas the pre-STI clusters (cluster A in patients 03 and 05 and cluster GG in patient 19) were generally located farther from the root. Additionally, the branch length leading to the root of post-STI clusters was shorter than the length of pre-STI clusters. In details, for patient 03 the branch length of the cluster M (pos-STI) was 0.00862 (± 0.002) whereas the branch length of the cluster A (pre-STI) was 0.03341 (± 0.005) (Fig. 4). For patient 05, the branch length of cluster I (post-STI) was 0.03155 (± 0.0034) and for cluster A (pre-STI) it was 0.05178 (± 0.004). Finally, for patient 19 the branch length of the clusters GW 1 and GW 2 (post-STI) was 0.01323 (± 0.007) and 0.03881 (± 0.006), respectively, whereas the branch length of the cluster GG (pre-STI) was 0.10195 (± 0.002). The above results showed steadily that the post-STI sequences diversified less than pre-STI sequences from the midpoint root.

To give more strength to our hypothesis of recrudescence of ancient variants, we used the coalescent approach to estimate “age” of the clusters. This analysis revealed that the clusters formed by post-STI sequences had reduced coalescent time intervals compared to those estimated for the clusters formed by pre-STI sequences. For patient 03, for example, the coalescent time interval for the cluster M was 0.025 substitutions whereas for the cluster A it was four times longer; 0.10 substitutions (Fig. 4, panels A and B, respectively). Likewise, for patient 05/cluster I, the coalescent time interval was 0.02 and there was no evidence of population growth, whereas for the cluster A the coalescent time interval was five times longer; 0.10 substitutions (Fig. 5, panels A and B, respectively). For patient 19, the coalescent time interval for clusters GW 1 and GW 2 was 0.04 and for the cluster GG was 0.05 (Fig. 6, panels A–C). These results revealed that clusters formed by post-STI sequences had shorter coalescent time interval than those observed in clusters formed by pre-STI sequences. Therefore, implying that even without assuming a midpoint root, the clusters of post-STI

sequences coalesced less from the ancestor, thus showing that the post-STI sequences are older than the pre-STI sequences. Data for patients 1 and 4 are not presented due to the relative homogeneity of their sequences pre- and post-STI.

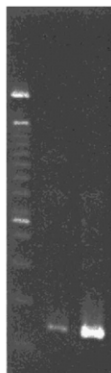
Discussion

In this study, we analyzed the genetic diversity of chronically HIV-1-infected patients failing antiretroviral therapy and subjected to STI. The preliminary analysis using HMA revealed no defined pattern of *env* evolution after antiretroviral interruption. It is interesting to note that, despite the selective pressure imposed by antiretroviral therapy, genetic diversity can vary widely in this gene. In addition, after interruption of the selective pressure exerted by the antiretroviral agents, there is a change in the genetic complexity of the gp120 V3 region of viruses over a short period of time in 17 out of 27 individuals, favoring either the increase or decrease of the genetic diversity of the virus. There have been few studies analyzing the impact of STI on genes other than *pol* (Kijak et al., 2002). Studies of the use of STI in patients failing antiretroviral therapy have shown that this strategy leads to an increase in viral load and a decrease in CD4

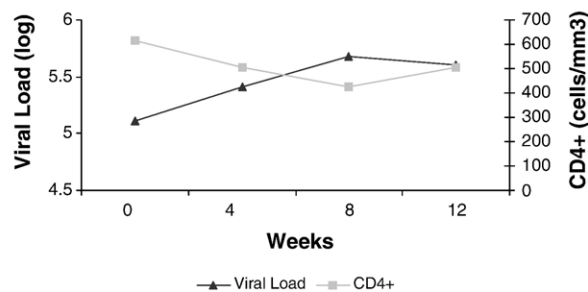
counts, as well as rapid replacement of viruses presenting resistance mutations in the *pol* gene by wild-type viruses (Deeks et al., 2001; Miller et al., 2000). These emerging wild-type viruses probably represent viral populations archived in reservoirs or sanctuaries and emerge due to their higher fitness in the absence of antiretroviral agents. Another related issue that needs to be taken into consideration is genomic recombination. One hypothesis is that despite the *pol* profile, the more highly adapted *env* should prevail. If this is true, recombination would result in the current *env* profile being maintained, even with the post-STI emergence of wild-type *pol* profile.

In order to make a more detailed evaluation, we used endpoint PCR to analyze the genetic profile of pre- and post-STI viral strains by sequencing clones amplified from samples obtained from five patients. As an initial screening method, HMA was used. Although not highly specific, HMA allows the rapid and inexpensive analysis of a large number of samples and has primarily been used for these applications (Delwart et al., 1993; Diaz et al., 1995; Long et al., 2000). Indeed, we found an interesting lack of concordance between the two methods in some of the five cases in which sequencing was performed. As mentioned earlier, in samples from patients 01, 03 and 05, there

Patient 01



Protease Codon	Amino Acid	
	Pre-STI	pos-STI
10	V	L
36	I	I
46	L	L
54	V	V
63	P	H
71	T	T
Transcriptase Codon	Pre-STI	pos-STI
	41	L
70	K	R
103	N	N
181	C	Y
184	V	M
190	A	G
215	Y	T



Patient 03



Protease Codon	Amino Acid	
	Pre-STI	pos-STI
10	L	I
20	K	R
24	I	L
36	I	I
48	R	V
53	L	F
54	V	V
63	P	L
77	I	I
82	I	V
Transcriptase Codon	Pre-STI	pos-STI
	41	L
67	K	D
70	R	K
181	C	Y
184	V	M
190	A	G
215	Y	T

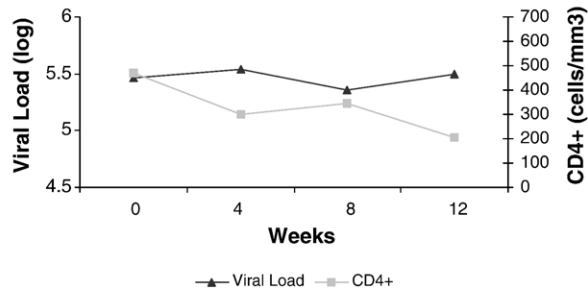
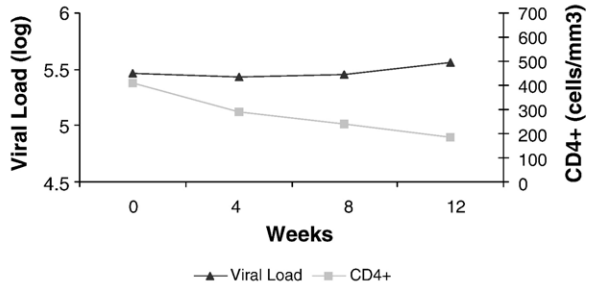


Fig. 2. HMA genetic diversity (left), resistance mutation codons (middle) and viral load/CD4 variation during the STI (right) for patients 01, 03, 04, 05 and 19. Amino acid substitutions are represented as single letter codes. Letters in black indicate wild-type viruses and letters in gray indicate mutant viruses. Along the y axis, viral loads are shown on the left, whereas CD4 counts are shown on the right.

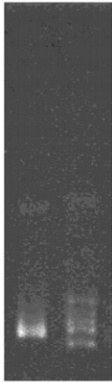
Patient 04



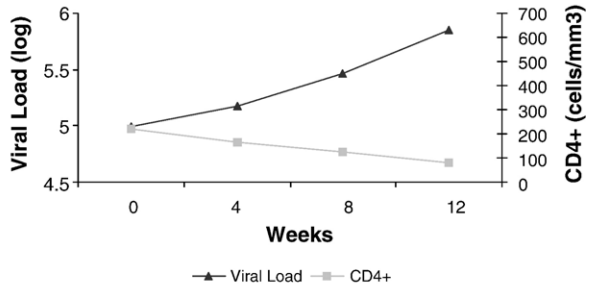
Protease Codon	Amino Acid	
	Pre-STI	pos-STI
10	R	L
20	R	K
36	I	M
48	V	G
54	V	I
63	L	A
71	T	M
82	A	V
88	N	D
Transcriptase Codon	Pre-STI	
	Pre-STI	pos-STI
67	N	D
181	C	Y
184	V	M
215	Y	T
219	Q	K



Patient 05



Protease Codon	Amino Acid	
	Pre-STI	pos-STI
20	I	K
46	M	I
63	P	L
Transcriptase Codon	Pre-STI	
	Pre-STI	pos-STI
41	L	M
70	R	R
181	C	Y
184	V	M
215	Y	T
219	Q	K



Patient 19



Protease Codon	Amino Acid	
	Pre-STI	pos-STI
20	R	R
36	I	I
54	V	V
63	P	P
71	V	V
82	A	V
88	S	N
90	M	M
Transcriptase Codon	Pre-STI	
	Pre-STI	pos-STI
41	L	L
44	D	D
67	N	K
118	I	I
181	C	C
184	V	V
190	A	A
210	W	W
215	Y	Y
219	N	N

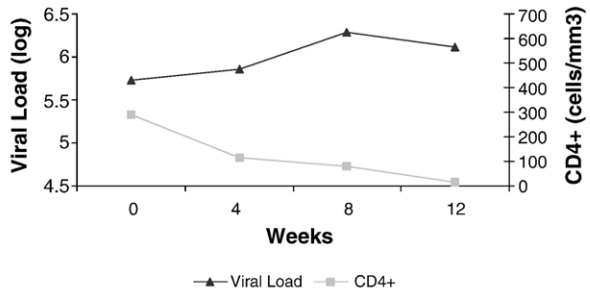


Fig. 2 (continued).

were strong correlations between the genetic diversity values inferred by HMA and those measured by sequencing. In the HMA, samples from patient 01 presented low genetic complexity before and after STI, which was in agreement with the sequencing results showing genetic diversity to be 0.32% in the pre-STI sample and 0.62% in the post-STI sample. The same occurred in patient 03 samples, which presented high pre-STI genetic diversity and low post-STI genetic diversity in the HMA,

which were 5.9% and 2.9%, respectively, in the sequencing. In the HMA, patient 05 samples presented low pre-STI genetic diversity and high post-STI genetic diversity, which were 1.8% and 8.1%, respectively, in the sequencing. However, samples from patients 04 and 19 presented genetic diversity values obtained through the use of the two methodologies that initially seem to be unrelated. The HMA of patient 04 samples classified the clones as presenting low pre-STI and high post-STI genetic

Patient 01

	C2		V3 loop					C3							
	270	280	290	300	306	310	320	330	340	350	360				
1A-01	LAEDEVVIRS	ENFTNNAKVI	IVQLNESVII	NCTRFNNNTR	KS	SIHI	GP	GS	SA	FYATG	DIIGD	IRQAHCNLSR	AQWNNLTKQI	VIKLREQPKN	KTIVFNQSS
DV 1A = 0.38%	1A-02	-----	-----	-----	-----	-----	-----	-----	-----	-----	-----	-----	-----	-----	-----
	1A-03	-----	-----	-----	-----	-----	-----	-----	-----	-----	-----	-----	-----	-----	-----
	1A-04	-----	-----	-----	-----	-----	-----	-----	-----	-----	-----	-----	-----	-----	-----
DV 1M = 0.62%	1A-05	-----	-----	-----	-----	-----	R	-----	-----	-----	-----	-----	-----	-----	-----
	1A-06	-----	-----	-----	-----	-----	-----	-----	-----	-----	-----	-----	-----	N	-----
	1A-07	-----	-----	-----	V	-----	-----	-----	-----	-----	-----	-----	-----	N	-----
DV 1A +1M = 0.46%	1A-08	-----	-----	-----	V	-----	-----	-----	-----	-----	-----	-----	-----	N	-----
	1A-09	-----	-----	-----	V	-----	-----	-----	-----	-----	-----	-----	-----	N	-----
	1A-10	-----	-----	-----	V	-----	-----	-----	-----	-----	-----	-----	-----	N	-----
dn/ds = 0.1973	1M-01	-----	-----	-----	-----	-----	-----	-----	-----	-----	-----	-----	-----	-----	-----
	1M-02	-----	-----	-----	-----	-----	-----	-----	-----	-----	-----	-----	-----	-----	-----
	1M-03	-----	-----	-----	V	-----	-----	-----	-----	-----	-----	-----	-----	-----	-----
Model = M0	1M-04	-----	-----	-----	-----	-----	-----	-----	-----	-----	-----	-----	-----	N	-----
	1M-05	-----	-----	-----	-----	-----	-----	-----	-----	-----	-----	-----	-----	N	-----
	1M-06	-----	-----	-----	-----	-----	-----	-----	-----	-----	-----	-----	-----	N	-----
	1M-07	-----	-----	-----	-----	-----	-----	-----	-----	-----	-----	-----	-----	N	A
	1M-08	-----	-----	-----	K	-----	-----	-----	-----	-----	-----	-----	-----	N	-----
	1M-09	-----	-----	-----	V	-----	-----	-----	-----	-----	-----	-----	-----	N	-----

Patient 03

	C2		V3 loop					C3					
	282	290	300	306	310	320	330	340	350	360			
3A-16	GSIIIVQLNES	VVINCTRPNN	NTRK	SIHM	GP	GGAFYTTG	ELIGNIRKAY	CTINGTEWNN	TLRRIVIKLQ	EQ	.FKNKAI	IFKQ	SSGGDP
DV 3A = 5.9%	3A-19	-----	-----	-----	-----	-----	-----	-----	-----	-----	-----	-----	-----
	3A-20	-----	-----	-----	-----	-----	-----	-----	-----	-----	-----	-----	-----
	3A-05	-----	-----	-----	-----	-----	-----	-----	-----	-----	-----	-----	-----
DV 3M = 2.9%	3A-06	-----	-----	-----	-----	-----	-----	-----	-----	-----	-----	-----	-----
	3A-07	-----	-----	-----	-----	-----	-----	-----	-----	-----	-----	-----	-----
	3A-61	-----	-----	-----	-----	-----	-----	-----	-----	-----	-----	-----	-----
DV 3A +3M = 5.2%	3A-04	-----	-----	-----	-----	-----	-----	-----	-----	-----	-----	-----	-----
	3A-10	-----	-----	-----	-----	-----	-----	-----	-----	-----	-----	-----	-----
	3A-14	-----	-----	-----	-----	-----	-----	-----	-----	-----	-----	-----	-----
dn/ds = [1]=0.297	3M-07	-----	-----	-----	-----	-----	-----	-----	-----	-----	-----	-----	-----
[2]=0.301 [3]=3.298	3M-09	-----	-----	-----	-----	-----	-----	-----	-----	-----	-----	-----	-----
Model = M2	3M-08	-----	-----	-----	-----	-----	-----	-----	-----	-----	-----	-----	-----
	3M-05	-----	-----	-----	-----	-----	-----	-----	-----	-----	-----	-----	-----
	3M-03	-----	-----	-----	-----	-----	-----	-----	-----	-----	-----	-----	-----
	3M-04	-----	-----	-----	-----	-----	-----	-----	-----	-----	-----	-----	-----
	3M-02	-----	-----	-----	-----	-----	-----	-----	-----	-----	-----	-----	-----
	3M-11	-----	-----	-----	-----	-----	-----	-----	-----	-----	-----	-----	-----
	3M-12	-----	-----	-----	-----	-----	-----	-----	-----	-----	-----	-----	-----
	3M-06	-----	-----	-----	-----	-----	-----	-----	-----	-----	-----	-----	-----
	3M-10	-----	-----	-----	-----	-----	-----	-----	-----	-----	-----	-----	-----

Patient 04

	C2		V3 Loop					C3				
	290	300	306	310	320	330	340	350	360			
4A-04	IIVQLNEAIE	INCTRPSNNT	RK	SIHI	GP	GR	AFYATGEIIG	DIRQAHCNLS	GAQWEKTLKQ	IATKLBQLG	EQFNNSIVFN	RSSGG
DV 4A = 1.1%	4A-10	-----	-----	-----	-----	-----	-----	-----	-----	-----	-----	-----
	4A-07	-----	-----	-----	-----	-----	-----	-----	-----	-----	-----	-----
DV 4J = 0.8%	4A-02	-----	-----	-----	-----	-----	-----	-----	-----	-----	-----	-----
	4A-08	-----	-----	-----	-----	-----	-----	-----	-----	-----	-----	-----
	4A-03	-----	-----	-----	-----	-----	-----	-----	-----	-----	-----	-----
DV 4A +4J = 0.9%	4A-05	-----	-----	-----	-----	-----	-----	-----	-----	-----	-----	-----
	4A-09	-----	-----	-----	-----	-----	-----	-----	-----	-----	-----	-----
	4A-01	-----	-----	-----	-----	-----	-----	-----	-----	-----	-----	-----
dn/ds = 0.4987	4A-06	-----	-----	-----	-----	-----	-----	-----	-----	-----	-----	-----
	4J-03	-----	-----	-----	-----	-----	-----	-----	-----	-----	-----	-----
	4J-02	-----	-----	-----	-----	-----	-----	-----	-----	-----	-----	-----
	4J-01	-----	-----	-----	-----	-----	-----	-----	-----	-----	-----	-----
Model = M0	4J-04	-----	-----	-----	-----	-----	-----	-----	-----	-----	-----	-----
	4J-06	-----	-----	-----	-----	-----	-----	-----	-----	-----	-----	-----
	4J-08	-----	-----	-----	-----	-----	-----	-----	-----	-----	-----	-----
	4J-05	-----	-----	-----	-----	-----	-----	-----	-----	-----	-----	-----
	4J-07	-----	-----	-----	-----	-----	-----	-----	-----	-----	-----	-----

Patient 05

	C2		V3 Loop					C3					
	280	290	300	306	310	320	330	340	350	360			
5A-05	SENITNNAKT	IIVHLNESVQ	INCTRPKNNT	IR	RIHI	GP	GR	AFYTTKLAGN	IRQAHCNLSS	TQWNNLQRI	VIKLREQFGD	KTMVFRPSSG	GDP
DV 5A = 1.8%	5A-09	-----	-----	-----	-----	-----	-----	-----	-----	-----	-----	-----	-----
	5A-04	-----	-----	-----	-----	-----	-----	-----	-----	-----	-----	-----	-----
	5A-03	-----	-----	-----	-----	-----	-----	-----	-----	-----	-----	-----	-----
DV 5L = 8.1%	5A-06	-----	-----	-----	-----	-----	-----	-----	-----	-----	-----	-----	-----
	5A-01	-----	-----	-----	-----	-----	-----	-----	-----	-----	-----	-----	-----
	5A-07	-----	-----	-----	-----	-----	-----	-----	-----	-----	-----	-----	-----
DV 5A + 5L = 4.2%	5A-02	-----	-----	-----	-----	-----	-----	-----	-----	-----	-----	-----	-----
	5A-10	-----	-----	-----	-----	-----	-----	-----	-----	-----	-----	-----	-----
	5A-08	-----	-----	-----	-----	-----	-----	-----	-----	-----	-----	-----	-----
dn/ds = [1]=0	5L-04	-----	-----	-----	-----	-----	-----	-----	-----	-----	-----	-----	-----
[2]=1 [3]=9.219	5L-10	-----	-----	-----	-----	-----	-----	-----	-----	-----	-----	-----	-----
Model = M2	5L-09	-----	-----	-----	-----	-----	-----	-----	-----	-----	-----	-----	-----
	5L-06	-----	-----	-----	-----	-----	-----	-----	-----	-----	-----	-----	-----
	5L-08	-----	-----	-----	-----	-----	-----	-----	-----	-----	-----	-----	-----
	5L-05	-----	-----	-----	-----	-----	-----	-----	-----	-----	-----	-----	-----
	5L-01	-----	-----	-----	-----	-----	-----	-----	-----	-----	-----	-----	-----
	5L-03	-----	-----	-----	-----	-----	-----	-----	-----	-----	-----	-----	-----
	5L-02	-----	-----	-----	-----	-----	-----	-----	-----	-----	-----	-----	-----
	5L-07	-----	-----	-----	-----	-----	-----	-----	-----	-----	-----	-----	-----

Fig. 3.

Patient 19

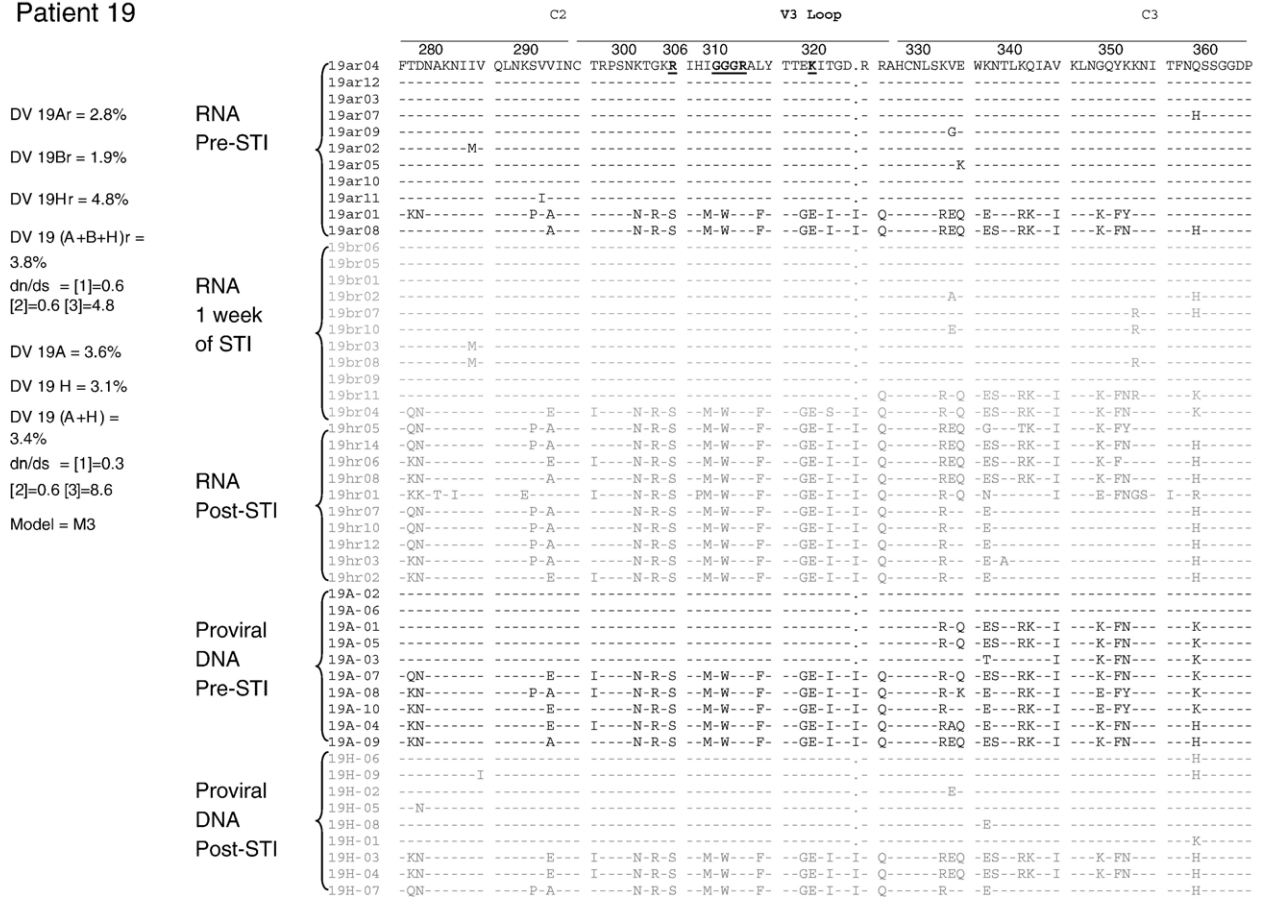


Fig. 3. Amino acid sequence alignments for the five patients analyzed. On the right, the genetic diversity (GD) found in pre-STI samples, 1 week of STI (for patient 19) and 12 weeks of STI (post-STI) is shown. The dN/dS ratios and model used for each estimation are indicated. Pre-STI sequences are at the top of the alignment, and post-STI sequences are at the bottom. Samples are labeled with a number representing the number of the clone generated by end-point PCR. All positive PCR clones were sequenced and included in this analysis. The sequence at the top is the consensus sequence for the quasispecies found in the samples obtained from each patient. Dots indicate similarities, whereas dashes indicate the absence of amino acids. The V3 loop, between the two cysteines, is indicated by the break in the upper line. In the alignment, positions 306 and 320, which predict viral phenotype, are marked in bold. For patient 19, alignments at the top are from RNA sequences, whereas the corresponding alignments at the bottom are from proviral DNA.

complexity. However, in the analysis of the sequencing results for the same samples, genetic diversity was low in pre- and post-STI samples (1.1% and 0.8%, respectively). Careful examination of the HMA of the post-STI sample revealed that there was only one heteroduplex band presenting slow migration rather than the smear of heteroduplexes closer to the homoduplexes seen in the other high genetic complexity samples. Interestingly, as seen in Fig. 3, the quasispecies infecting this patient presented sequences with a deletion. The HMA showed that this deletion, although not influencing the amount of genetic diversity calculated from the sequences, resulted in anomalous annealing, which in turn led to slower migration of the heteroduplexes. In the HMA of patient 19 samples, we found high initial genetic diversity and low final genetic diversity, whereas the sequencing revealed 3.6% and 3.1%, respectively. Although there was a discrete decrease in post-STI genetic diversity, we considered genetic diversity to be high at both time points. This patient was especially interesting because, in addition to the conflict between HMA and sequencing results, there was also a significant increase in viral load and a decrease in the CD4

count, despite the fact that the wild-type virus did not emerge after STI. The *pol* gene mutations led to a high level of genotypic antiretroviral resistance. After STI, the patient did not revert to wild type, either at the provirus (PBMC) or virion (plasma) level. All other patients reverted to wild-type mutations after STI, and the *pol* provirus profile of patient 19 was similar to that found in the plasma of all patients (data not shown). These results motivated us to evaluate this patient in greater detail. To that end, we analyzed the V3 quasispecies viruses present in plasma and included one sample obtained after 1 week of STI.

The sequence analysis produced very interesting results. Patient 01 did not present any change in the *env* sequence profile after STI, despite the changes presented in the *pol* gene. The proviral population remained homogeneous with extremely low selective positive pressure, denoting the low immune pressure exerted by this antigenic stimulus (Fig. 3). The results from patient 04 are similar to those obtained for patient 01. In contrast, patient 03 samples presented a significant post-STI decrease in genetic diversity. It is of note that the majority of pre-STI strains presented characteristics consistent with ×4 strains (SI

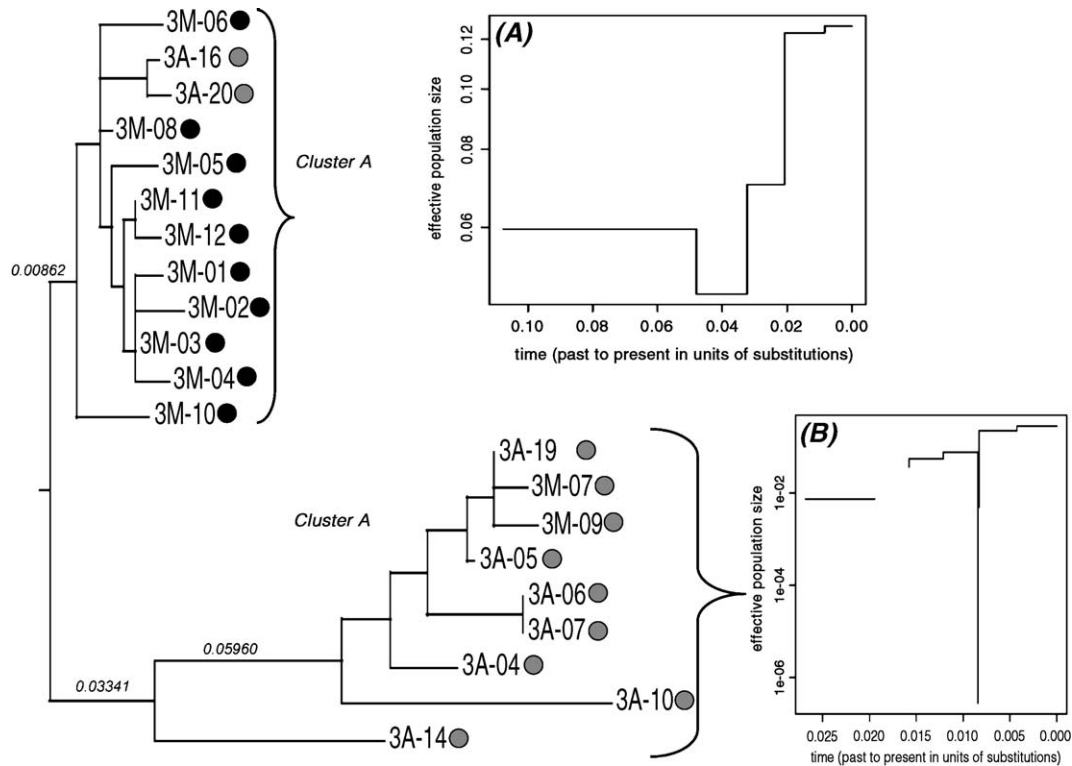


Fig. 4. Maximum likelihood tree and coalescent intervals of gp120 V3 *env* region of patient 03. The STI status of the sequences are identified with circles: sequences isolated from the pre-STI time point are grey circles, whereas sequences obtained from the post-STI time point are black circles. The tree was rooted at its midpoint; the topology clustered the sequences in two distinct groups, labeled as clusters A and M. The cluster A includes most of pre-STI sequences whereas cluster M includes most of Post-STI sequences. Numbers above the branches are length of clusters to the root. To the right side of the tree, the panels describe the Bayesian skyline plot depicting the coalescent intervals of each cluster. The x axis is in units of time (substitutions). The y axis represents the effective population size. Hence, panel A is the coalescent interval of cluster M and panel B is the coalescent interval of the cluster A.

phenotype), as predicted by the presence of amino acids with positive charges at position 306 or 320 of the V3 loop (R or K). After STI, these strains were replaced by strains presenting amino acids with neutral charges at position 306 (S) or negative charges at position 320 (E), which is typical of R5 NSI strains (Fouchier et al., 1992). It is recognized that $\times 4$ strains do not usually appear in the early stages of HIV-1 infection, typically arising and replacing the R5 strains in the advanced stages of the disease. We therefore believe that this patient was in the advanced stages of the disease when antiretroviral therapy was started, and that, after STI, there was a reemergence of strains that had been present in the early stages of the disease, together with the reemergence of wild-type *pol* gene. In addition, selective pressure, as inferred by the dN/dS ratios, was high in the strains found in patient 03 samples.

More interesting still is the phenomenon seen in patient 05. As seen in patient 03 samples, the pre-STI patient 05 samples presented exclusively $\times 4$ strains (R at position 306), and the post-STI patient 05 samples presented a mixed population of $\times 4$ and R5 strains in similar proportions, some strains maintaining a positive charge at position 306 and others maintaining a neutral charge at this position. This mixed viral population was also responsible for the increase in genetic diversity in the post-STI sample. In this patient, selective pressure was also high, as evidenced by the high rates of non-

synonymous substitutions, which sustained the high dN/dS ratio. It is likely that recombination is the mechanism by which the more recent ($\times 4$) strains coexist with the more ancient, reemerged (R5) strains. This scenario was repeated in the case of patient 19. The phenomenon was more pronounced from the sequencing of virus samples obtained as actively replicating virions that were shed in the blood stream. The pre-STI strains were $\times 4$ strains, presenting K at positions 306 and 320, and these strains were replaced by R5 strains presenting neutral (S) amino acids at position 306, or negative (E) amino acids at position 320 after STI. In addition, pre-STI strains presented a GGGR motif at the tip of the V3 loop, which was replaced by a GWGR motif after STI. It is known that GWGR is the typical motif found in a proportion of Brazilian clade B strains (Hendry et al., 1996; Morgado et al., 1994), and that, due to the instability of the tryptophan in this position, this motif tends to disappear over the course of HIV infection. Tryptophan is typically replaced by amino acids, such as glycine, that are genetically closer to tryptophan. The reemergence of strains with the GWGR motif provides further evidence that the more recent strains were replaced by older strains. As previously mentioned, although patient 19 was the only patient that did not revert the antiretroviral resistance-related viral mutations to wild type, either in the plasma or in the PBMC, there was a significant increase in viral load after

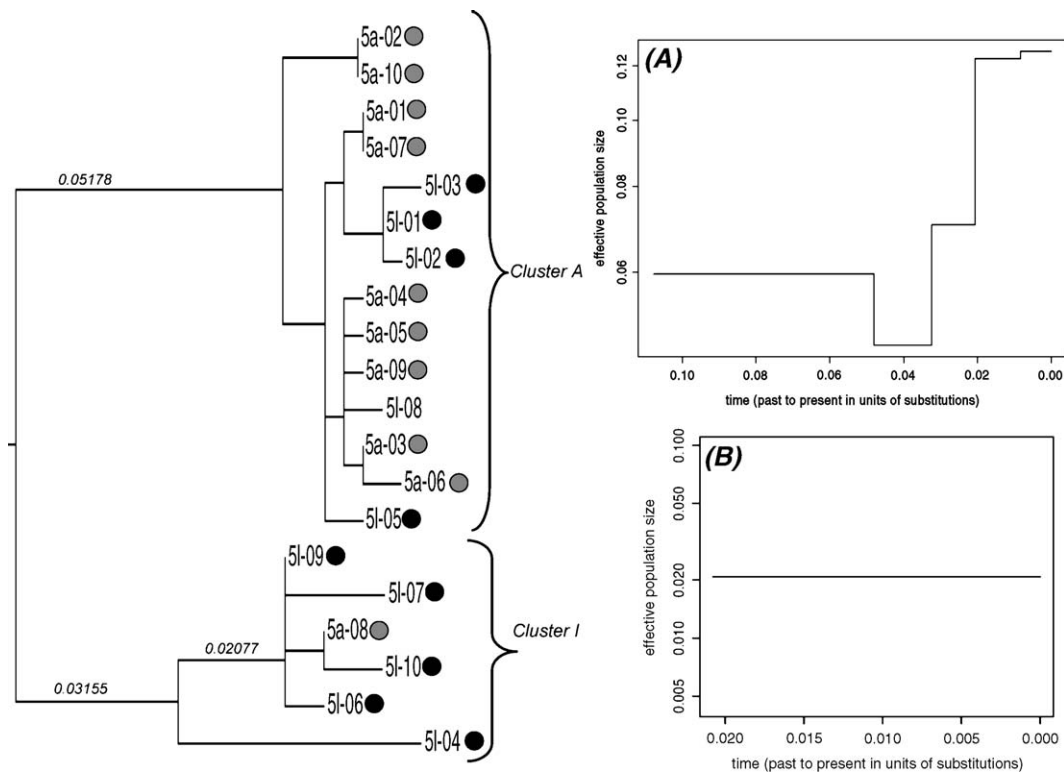


Fig. 5. Maximum likelihood tree and coalescent intervals of gp120 V3 *env* region of patient 05. The STI status of the sequences is identified with circles: sequences isolated from the pre-STI time point are grey circles, whereas sequences obtained from the post-STI time point are black circles. The tree was rooted at its midpoint; the topology clustered the sequences in two distinct groups, labeled as clusters A and I. The cluster A includes most of pre-STI sequences whereas cluster I includes most of Post-STI sequences. Numbers above the branches are length of clusters to the root. To the right side of the tree, the panels describe the Bayesian skyline plot depicting the coalescent intervals of each cluster. The x axis is in units of time (substitutions). The y axis represents the effective population size. Hence, panel A is the coalescent interval of cluster A and panel B is the coalescent interval of the cluster I.

STI. This suggests that although there was broad antiretroviral resistance due to the presence of resistance mutations, these medications might have a residual antiretroviral effect on viral suppression.

It is also of note that, after STI, CD4 counts did not always change in ways that were proportional to post-STI changes in viral loads. In patients 03 and 04, there was no significant increase in viral loads after 12 weeks of STI, although CD4 counts decreased by more than 50%. The unique feature in these two cases was the reemergence of the wild-type strains. In both of these cases, there was an increase in viral activation after STI (data not shown). One could therefore speculate that the massive cell destruction was related to the cell activation caused by the emergence of wild-type viruses and not to the direct cytopathic effect of the high viral loads (Smith et al., 2002).

One possible limitation of our study is the fact that we analyzed the provirus quasispecies rather than the viral quasispecies. Indeed, RNA analysis could have increased the sensitivity to the more dynamic changes in the viral quasispecies, such as those seen in patient 19 samples. However, our focus was the impact of these changes on the cellular reservoir of these patients. Studies of HIV-1 dynamics have indicated that because the half-life of more than 99% HIV-infected cells is approximately 2.4 days, the time required to seed the cell reservoir is extremely short (Ho, 1995; Wei et al., 1995).

Our study therefore provides unique and interesting insights into aspects of the dynamics of HIV-1 viral replication in humans. We demonstrated that the dramatic disturbance caused by the interruption of antiretroviral therapy results in the activation of old progenies that are able to repopulate the patient's cell reservoir. However, there were two patients in whom this phenomenon was not observed. These two patients presented highly homogeneous sequences and low immune selective pressure, as inferred by the dN/dS ratios <1. We have developed three separate hypotheses regarding these two cases. First, these patients might have been treated early, before significant genetic diversity was acquired, thereby presenting only one viral profile in the quasispecies. Second, as has previously been suggested (Wolinsky et al., 1996), low selective pressure due to a weak immune system might have precluded the generation of significant genetic diversity, again resulting in a single viral profile. Third, as proposed by Costa et al. (2004), because the change in the *pol* profile in these two cases suggested that the best adapted *env* profile to the patient at this time would be the current one, recombination might have maintained the genetic *env* profile after STI. Indeed, there is some evidence that recombination may have occurred in patient 05. In patient 05 samples, we detected two distinct viral populations after STI: one being a more ancient, emerging population; and the other presenting similar proportions of

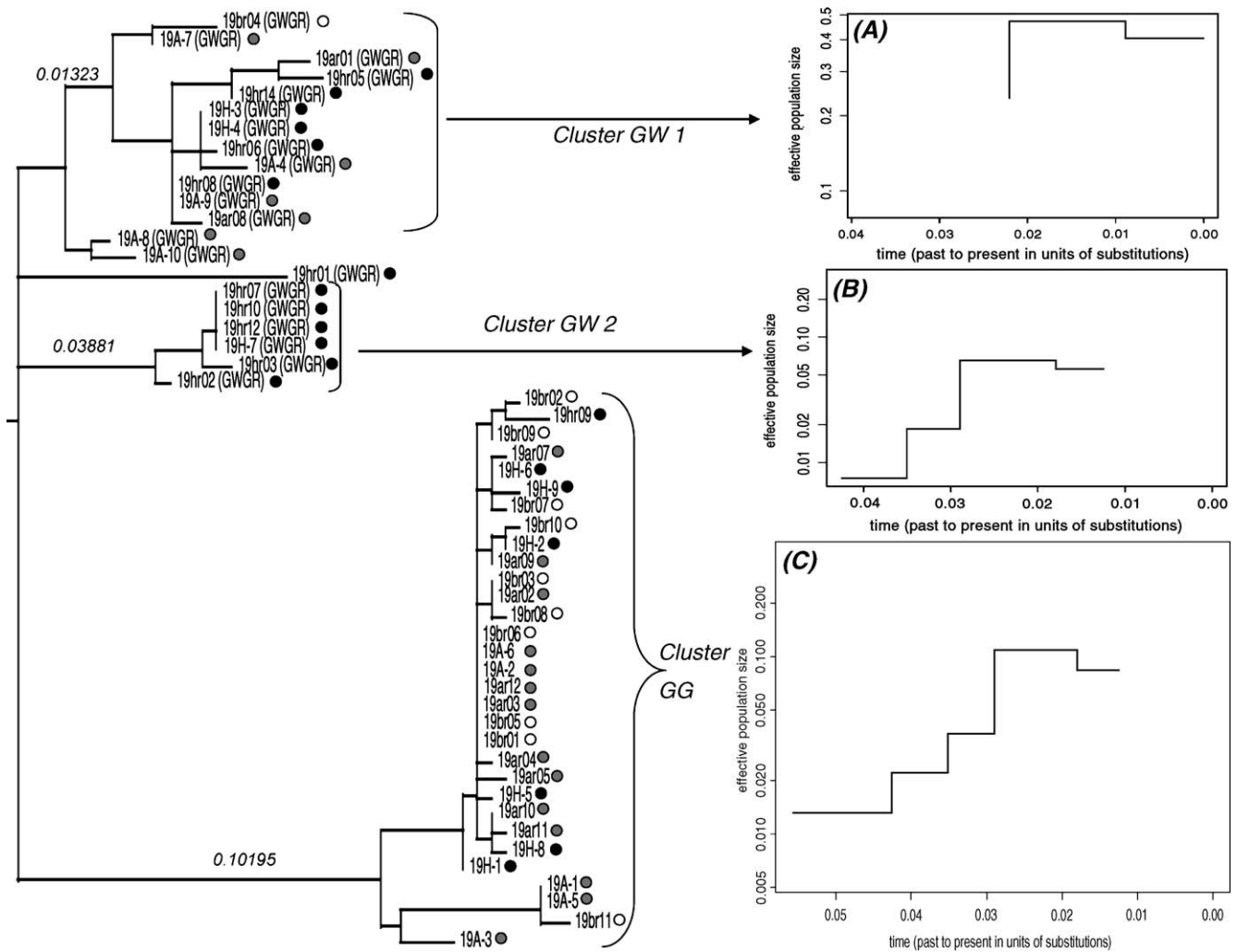


Fig. 6. Maximum likelihood tree and coalescent intervals of gp120 V3 *env* region of patient 19. The STI status of the sequences are identified with circles: sequences isolated from the pre-STI time point are grey circles, sequences obtained 1 week after STI are white circles and sequences obtained 12 weeks after STI are black circles. The tree was rooted at its midpoint; the topology clustered the sequences in two distinct groups, labeled as clusters GG (presenting the motif GGGR at the tip of the V3 loop) and GW (GW 1 and GW 2, presenting the GWGR motif at the tip of the V3 loop). The cluster GG includes most of pre-STI sequences whereas cluster GW includes most of post-STI sequences. Numbers above the branches are length of clusters to the root. To the right side of the tree, the panels describe the Bayesian skyline plot depicting the coalescent intervals of each cluster. The x axis is in units of time (substitutions). The y axis represents the effective population size. Hence, panels A and B are the coalescent interval of cluster GW 1 and GW 2, respectively, and panel C is the coalescent interval of the cluster GG.

ancient and recent strains. Our findings provide insights into some of the mechanisms involved in viral evolution, in which selective pressure is applied not only by the immune system but also by antiretroviral therapy. Therefore, one outcome of STI for patients could be the impact on the coreceptor usage of circulating viruses, leading to the suppression of $\times 4$ strains.

Methods

Sample collection

Samples to be analyzed were collected from 27 chronically infected patients who had experienced antiretroviral therapy failure and were subjected to an STI at the Universidade Federal de São Paulo, Brazil, between June 1999 and June 2000. All

samples were obtained from peripheral blood mononuclear cells (PBMCs), except for select samples obtained from an individual patient, which were derived from plasma.

Nucleic acid purification

The HIV-1 proviral DNA was extracted from buffy coats using the QIAamp DNA Blood Mini Kit (Qiagen Inc., Santa Clarita, CA), and viral RNA was purified from plasma using the QIAamp viral RNA kit (Qiagen) according to the manufacturer instructions.

cDNA synthesis

Following RNA viral denaturation at 70 °C for 10 min, cDNA synthesis was performed at 42 °C for 90 min using a

reverse transcriptase enzyme (20 U Super Script TM II; Gibco BRL-Life Technologies, Rockville, MD).

Nested PCR amplification

A C2-V3-C3 region 300-bp fragment (designated V3 for the sake of simplicity) was amplified using nested PCR as previously described (Wolfs et al., 1991). For the *pol* gene amplification, we used a nested PCR as previously described (Sucupira et al., 2001).

Heteroduplex mobility analysis

After PCR amplification, samples were screened using heteroduplex mobility analysis (HMA) (Delwart et al., 1993). The V3 PCR products were denatured at 94 °C for 2 min, chilled on ice and subjected to electrophoresis on a polyacrylamide gel as previously described (Diaz et al., 1999).

End-point PCR

The strategy for generating PCR clones was based on serial dilutions of DNA samples. An aliquot of the last dilution in which there was positive amplification was added to a PCR mixture (total volume of 1 mL), which was then divided among 20 reaction tubes (50 µL per tube). If the number of positive amplifications was that expected from the Poisson distribution (the probability of each amplification event starting from a single template and inversely proportional to the number of events), the positive amplification products were considered clones (Diaz et al., 1995; Simmonds et al., 1990).

DNA sequencing

The PCR products were purified using the QIAquick PCR Purification Kit® (Qiagen Inc., Chatsworth, CA) according to manufacturer instructions.

Sequencing was performed using the Thermo Sequenase Fluorescent-labeled primer cycle sequencing kit (RPN 2436; Amersham Pharmacia Biotech UK Limited, Buckinghamshire, England), and primers were labeled with CY5.5. Electrophoresis was performed using the Long Reader Tower (Bayer Corp., Berkeley, CA).

Predicting the HIV-1 phenotype

The *env* sequences corresponding to the V3 loop region were used to predict the coreceptor use and the viral phenotype based on the presence of residues at positions 306 and 320 in the V3 loop (Chesebro et al., 1991; De Jong et al., 1992; Milich et al., 1993).

Genetic diversity

Patient sequences were aligned by eye using the SeaView (Galtier et al., 1996). The Modeltest program (Posada and Crandall, 1998) was used to select maximum likelihood models

of nucleotide substitutions for each alignment, and corrected distance matrices were then built using the PAUP* program [Swofford, DL (2002) PAUP*; Phylogenetic analysis using parsimony (*and other methods), Version 4; Sinauer Associates, Sunderland, MA]. Genetic diversity was calculated as

$$d = \sum_{ij} p_{ij} / n_c,$$

where p is the corrected distance between sequences i and j , and n_c is the total number of sequence comparisons among n sequences (Nei, 1987):

$$n_c = n(n-1)/2.$$

Selection pressures

Evidences that support selective pressure on the V3 region comes from the analysis of the dN/dS ratio of sequence pairs, where dN is the observed frequency of non-synonymous substitution per replacement site, and the dS is the observed frequency of synonymous substitution per silent site. The higher the dN/dS ratio (>1), the stronger the selective pressure for amino acid change. Phylogenetic trees for each patient were inferred by maximum likelihood using the PAUP* program, and for each alignment and correspondent tree, three models of codon substitution were compared using a likelihood ratio test (LRT) using CODEML as implemented in the PAML package [Yang, 1997; Phylogenetic Analysis by Maximum Likelihood (PAML), Version 1.4. department of Integrative Biology, University of California, Berkeley]. The first model, M0, assumes that all codons fall into a single category of sites with fixed non-synonymous to synonymous substitutions (dN/dS) ratios (Goldman and Yang, 1994). The second model, M1, assumes a class of conserved sites with dN/dS ratios equals 0 and a class of neutral sites with dN/dS = 1. The third model, M2, comprises the categories used in the second model and adds an additional category of positively selected sites with dN/dS >1 (Nielsen and Yang, 1998). An LRT was performed to compare the M0 and M1 models. When M1 was chosen, another LRT was applied to compare it with M2. When M2 was chosen, positively selected sites were identified by their posterior probabilities, as calculated by CODEML, of belonging to the class of sites presenting dN/dS ratios >1.

Alignment and phylogenetic inference

The sequences were manually aligned using the SE-AL program (Version 2.0; Department of Zoology, Oxford University [<http://evolve.zoo.ox.ac.uk/software/>]). Phylogenetic inferences were made using gp120 V3 *env* region of HIV-1. Maximum likelihood trees were done by first determining the most appropriate model of nucleotide substitution for each data set, according to a hierarchical likelihood ratio test (hLRT), as implemented in the program Modeltest v3.06 (Posada and Crandall, 1998). The most appropriate evolutive model was used to obtain the initial trees through the neighbor-joining method; the resulting trees were then swapped by the

nearest-neighbor interchange method (NNI). All phylogenetic inferences were done using the program PAUP*. To the coalescent analysis, we used the reversible jump Markov chain Monte Carlo method (Opgen-Rhein et al., 2005) as implemented in the “ape” library of the R-package (<http://www.r-project.org>).

Acknowledgments

This study received financial support from the Fundação de Amparo à Pesquisa do Estado de São Paulo (FAPESP, Foundation for the Support of Research in the State of São Paulo; grant number: 98/14381-4).

References

- Cheng-Mayer, C., Quiroga, M., Tung, J.W., Dina, D., Levy, J.A., 1990. Viral determinants of human immunodeficiency virus type 1 T-cell or macrophage tropism, cytopathogenicity, and CD4 antigen modulation. *J. Virol.* 64 (9), 4390–4398.
- Chesebro, B., Nishio, J., Perryman, S., Cann, A., O’Brien, W., Chen, I.S., Wehrly, K., 1991. Identification of human immunodeficiency virus envelope gene sequences influencing viral entry into CD4-positive HeLa cells, T-leukemia cells, and macrophages. *J. Virol.* 65 (11), 5782–5789.
- Coffin, J.M., 1995. HIV population dynamics in vivo: implications for genetic variation, pathogenesis, and therapy. *Science* 267 (5197), 483–489.
- Costa, L.J., Mayer, A.J., Busch, M.P., Diaz, R.S., 2004. Evidence for selection of more adapted human immunodeficiency virus type 1 recombinant strains in a dually infected transfusion recipient. *Virus Genes* 28 (3), 259–272.
- De Jong, J.J., De Ronde, A., Keulen, W., Tersmette, M., Goudsmit, J., 1992. Minimal requirements for the human immunodeficiency virus type 1 V3 domain to support the syncytium-inducing phenotype: analysis by single amino acid substitution. *J. Virol.* 66 (11), 6777–6780.
- Deeks, S.G., Wrin, T., Liegler, T., Hoh, R., Hayden, M., Barbour, J.D., Hellmann, N.S., Petropoulos, C.J., McCune, J.M., Hellerstein, M.K., Grant, R.M., 2001. Virologic and immunologic consequences of discontinuing combination antiretroviral-drug therapy in HIV-infected patients with detectable viremia. *N. Engl. J. Med.* 344 (7), 472–480.
- Delwart, E.L., Shpaer, E.G., Louwagie, J., McCutchan, F.E., Grez, M., Rubsamen-Waigmann, H., Mullins, J.I., 1993. Genetic relationships determined by a DNA heteroduplex mobility assay: analysis of HIV-1 *env* genes. *Science* 262 (5137), 1257–1261.
- Diaz, R.S., Sabino, E.C., Mayer, A., Mosley, J.W., Busch, M.P., 1995. Dual human immunodeficiency virus type 1 infection and recombination in a dually exposed transfusion recipient. The Transfusion Safety Study Group. *J. Virol.* 69 (6), 3273–3281.
- Diaz, R.S., Sabino, E.C., Mayer, A., deOliveira, C.F., Mosley, J.W., Busch, M.P., 1996. Lack of dual HIV infection in a transfusion recipient exposed to two seropositive blood components. *AIDS Res. Hum. Retrovir.* 12 (13), 1291–1295.
- Diaz, R.S., Zhang, L., Busch, M.P., Mosley, J.W., Mayer, A., 1997. Divergence of HIV-1 quasispecies in an epidemiologic cluster. *AIDS* 11 (4), 415–422.
- Diaz, R.S., De Oliveira, C.F., Pardini, R., Operskalski, E., Mayer, A.J., Busch, M.P., 1999. HIV type 1 *tat* gene heteroduplex mobility assay as a tool to establish epidemiologic relationships among HIV type 1-infected individuals. *AIDS Res. Hum. Retrovir.* 15 (13), 1151–1156.
- Fouchier, R.A., Groenink, M., Kootstra, N.A., Tersmette, M., Huisman, H.G., Miedema, F., Schuitemaker, H., 1992. Phenotype-associated sequence variation in the third variable domain of the human immunodeficiency virus type 1 gp120 molecule. *J. Virol.* 66 (5), 3183–3187.
- Galtier, N., Gouy, M., Gautier, C., 1996. SEAVIEW and PHYLO_WIN: two graphic tools for sequence alignment and molecular phylogeny. *Comput. Appl. Biosci.* 12 (6), 543–548.
- Goldman, N., Yang, Z., 1994. A codon-based model of nucleotide substitution for protein-coding DNA sequences. *Mol. Biol. Evol.* 11 (5), 725–736.
- Goudsmit, J., de Ronde, A., de Rooij, E., de Boer, R., 1997. Broad spectrum of in vivo fitness of human immunodeficiency virus type 1 subpopulations differing at reverse transcriptase codons 41 and 215. *J. Virol.* 71 (6), 4479–4484.
- Hendry, R.M., Hanson, C.V., Bongertz, V., Morgado, M., Duarte, A., Casseb, J., Brigido, L., Sabino, E., Diaz, R., Galvao-Castro, B., 1996. Immunoreactivity of Brazilian HIV isolates with different V3 motifs. *Mem. Inst. Oswaldo Cruz* 91 (3), 347–348.
- Ho, D.D., 1995. HIV-1 dynamics in vivo. *J. Biol. Regul. Homeostatic Agents* 9 (3), 76–77.
- Kijak, G.H., Simon, V., Balfe, P., Vanderhoeven, J., Pampuro, S.E., Zala, C., Ochoa, C., Cahn, P., Markowitz, M., Salomon, H., 2002. Origin of human immunodeficiency virus type 1 quasispecies emerging after antiretroviral treatment interruption in patients with therapeutic failure. *J. Virol.* 76 (14), 7000–7009.
- Koot, M., van ’t Wout, A.B., Kootstra, N.A., de Goede, R.E., Tersmette, M., Schuitemaker, H., 1996. Relation between changes in cellular load, evolution of viral phenotype, and the clonal composition of virus populations in the course of human immunodeficiency virus type 1 infection. *J. Infect. Dis.* 173 (2), 349–354.
- Larder, B.A., Kemp, S.D., 1989. Multiple mutations in HIV-1 reverse transcriptase confer high-level resistance to zidovudine (AZT). *Science* 246 (4934), 1155–1158.
- Long, E.M., Martin, H.L., Kreiss Jr., J.K., Rainwater, S.M., Lavreys, L., Jackson, D.J., Rakwar, J., Mandaliya, K., Overbaugh, J., 2000. Gender differences in HIV-1 diversity at time of infection. *Nat. Med.* 6 (1), 71–75.
- Maeda, Y., Venzon, D.J., Mitsuya, H., 1998. Altered drug sensitivity, fitness, and evolution of human immunodeficiency virus type 1 with *pol* gene mutations conferring multi-dideoxynucleoside resistance. *J. Infect. Dis.* 177 (5), 1207–1213.
- Mansky, L.M., Temin, H.M., 1995. Lower in vivo mutation rate of human immunodeficiency virus type 1 than that predicted from the fidelity of purified reverse transcriptase. *J. Virol.* 69 (8), 5087–5094.
- Martinez-Picado, J., Savara, A.V., Shi, L., Sutton, L., D’Aquila, R.T., 2000. Fitness of human immunodeficiency virus type 1 protease inhibitor-selected single mutants. *Virology* 275 (2), 318–322.
- McNearney, T., Hornickova, Z., Markham, R., Birdwell, A., Arens, M., Saah, A., Ratner, L., 1992. Relationship of human immunodeficiency virus type 1 sequence heterogeneity to stage of disease. *Proc. Natl. Acad. Sci. U.S.A.* 89 (21), 10247–10251.
- Milich, L., Margolin, B., Swanstrom, R., 1993. V3 loop of the human immunodeficiency virus type 1 Env protein: interpreting sequence variability. *J. Virol.* 67 (9), 5623–5634.
- Miller, V., Sabin, C., Hertogs, K., Bloor, S., Martinez-Picado, J., D’Aquila, R., Larder, B., Lutz, T., Gute, P., Weidmann, E., Rabenau, H., Phillips, A., Staszewski, S., 2000. Virological and immunological effects of treatment interruptions in HIV-1 infected patients with treatment failure. *AIDS* 14 (18), 2857–2867.
- Morgado, M.G., Sabino, E.C., Shpaer, E.G., Bongertz, V., Brigido, L., Guimaraes, M.D., Castilho, E.A., Galvao-Castro, B., Mullins, J.I., Hendry, R.M., et al., 1994. V3 region polymorphisms in HIV-1 from Brazil: prevalence of subtype B strains divergent from North American/European prototype and detection of subtype F. *AIDS Res. Hum. Retrovir.* 10 (5), 569–576.
- Nei, M., 1987. *Molecular Evolutionary Genetics*. Columbia Univ. Press, New York.
- Nielsen, R., Yang, Z., 1998. Likelihood models for detecting positively selected amino acid sites and applications to the HIV-1 envelope gene. *Genetics* 148 (3), 929–936.
- Opgen-Rhein, R., Fahmeir, L., Strimmer, K., 2005. Inference of demographic history from genealogical trees using reversible jump Markov chain Monte Carlo. *BMC Evolut. Biol.* 5 (6), 1–13.
- Perelson, A.S., Neumann, A.U., Markowitz, M., Leonard, J.M., Ho, D.D., 1996. HIV-1 dynamics in vivo: virion clearance rate, infected cell life-span, and viral generation time. *Science* 271 (5255), 1582–1586.
- Posada, D., Crandall, K.A., 1998. MODELTEST: testing the model of DNA substitution. *Bioinformatics* 14 (9), 817–818.

- Roos, M.T., Lange, J.M., de Goede, R.E., Coutinho, R.A., Schellekens, P.T., Miedema, F., Tersmette, M., 1992. Viral phenotype and immune response in primary human immunodeficiency virus type 1 infection. *J. Infect. Dis.* 165 (3), 427–432.
- Shankarappa, R., Margolick, J.B., Gange, S.J., Rodrigo, A.G., Upchurch, D., Farzadegan, H., Gupta, P., Rinaldo, C.R., Learn, G.H., He, X., Huang, X.L., Mullins, J.I., 1999. Consistent viral evolutionary changes associated with the progression of human immunodeficiency virus type 1 infection. *J. Virol.* 73 (12), 10489–10502.
- Simmonds, P., Balfe, P., Peutherer, J.F., Ludlam, C.A., Bishop, J.O., Brown, A.J., 1990. Human immunodeficiency virus-infected individuals contain provirus in small numbers of peripheral mononuclear cells and at low copy numbers. *J. Virol.* 64 (2), 864–872.
- Smith, K.Y., Steffens, C.M., Truckenbrod, A., Landay, A., Al-Harthi, L., 2002. Immune reconstitution after successful treatment with protease inhibitor-based and protease inhibitor-sparing antiretroviral regimens. *J. Acquired Immune Defic. Syndr.* 29 (5), 544–545.
- Sucupira, M.C., Souza, I.E., Costa, L.J., Scheinberg, M.A., Diaz, R.S., 2001. Antiretroviral treatment failure and HIV-1 genotypic resistance in Sao Paulo, Brazil. *Antiviral Therapy.* 6 (4), 263–264.
- Wei, X., Ghosh, S.K., Taylor, M.E., Johnson, V.A., Emini, E.A., Deutsch, P., Lifson, J.D., Bonhoeffer, S., Nowak, M.A., Hahn, B.H., et al., 1995. Viral dynamics in human immunodeficiency virus type 1 infection. *Nature* 373 (6510), 117–122.
- Wolfs, T.F., Zwart, G., Bakker, M., Valk, M., Kuiken, C.L., Goudsmit, J., 1991. Naturally occurring mutations within HIV-1 V3 genomic RNA lead to antigenic variation dependent on a single amino acid substitution. *Virology* 185 (1), 195–205.
- Wolinsky, S.M., Korber, B.T., Neumann, A.U., Daniels, M., Kunstman, K.J., Whetsell, A.J., Furtado, M.R., Cao, Y., Ho, D.D., Safrit, J.T., 1996. Adaptive evolution of human immunodeficiency virus-type 1 during the natural course of infection. *Science* 272 (5261), 537–542.
- Yang, Z., 1997. Phylogenetic Analysis by Maximum Likelihood (PAML), Version 1.4. Department of Integrative Biology, University of California, Berkeley.
- Zhang, L.Q., MacKenzie, P., Cleland, A., Holmes, E.C., Brown, A.J., Simmonds, P., 1993. Selection for specific sequences in the external envelope protein of human immunodeficiency virus type 1 upon primary infection. *J. Virol.* 67 (6), 3345–3356.
- Zhang, L., Diaz, R.S., Ho, D.D., Mosley, J.W., Busch, M.P., Mayer, A., 1997. Host-specific driving force in human immunodeficiency virus type 1 evolution in vivo. *J. Virol.* 71 (3), 2555–2561.
- Zhu, T., Mo, H., Wang, N., Nam, D.S., Cao, Y., Koup, R.A., Ho, D.D., 1993. Genotypic and phenotypic characterization of HIV-1 patients with primary infection. *Science* 261 (5125), 1179–1181.